Impact of Therapy on Genomics and Transcriptomics in High-Risk Prostate Cancer Treated with Neoadjuvant Docetaxel and Androgen Deprivation Therapy

Himisha Beltran[1], Alexander W. Wyatt[2], Edmund C. Chedgy[2], Adam Donoghue[1], Matti Annala[3], Evan W. Warner[2], Kevin Beja[2], Michael Sigouros[1], Fan Mo[2], Ladan Fazli[2], Colin C. Collins[2], James Eastham[4], Michael Morris[5], Mary-Ellen Taplin[6], Andrea Sboner[7,8], Susan Halabi[9], and Martin E. Gleave[2]

Abstract

Purpose: The combination of docetaxel chemotherapy and androgen deprivation therapy (ADT) has become a standard treatment for patients with metastatic prostate cancer. The recently accrued phase III CALGB 90203 trial was designed to investigate the clinical effectiveness of this treatment approach earlier in the disease. Specimens from this trial offer a unique opportunity to interrogate the acute molecular response to docetaxel and ADT and identify potential biomarkers.

Experimental Design: We evaluated baseline clinical data, needle biopsies, and radical prostatectomy (RP) specimens from 52 (of 788) patients enrolled on CALGB 90203 at one high volume center. Pathology review, tumor and germline-targeted DNA sequencing ($n = 72$ genes), and expression profiling using NanoString platform ($n = 163$ genes) were performed to explore changes in critical prostate cancer pathways linked to aggression and resistance.

Results: Three of 52 patients had only microfocal residual cancer at prostatectomy. The most common alterations included *TMPRSS2-ERG* fusion ($n = 32$), *TP53* mutation or deletion ($n = 11$), *PTEN* deletion ($n = 6$), *FOXA1* ($n = 6$), and *SPOP* ($n = 4$) mutation, with no significant enrichment in posttreated specimens. We did not observe *AR* amplification or mutations. The degree of AR signaling suppression varied among treated tumors and there was upregulation of both AR and AR-V7 expression as well as a subset of neuroendocrine and plasticity genes.

Conclusions: These data support the feasibility of targeted and temporal genomic and transcriptome profiling of neoadjuvant-treated prostate cancer with limited formalin-fixed paraffin embedded tissue requirement. Characterization of the heterogeneity of treatment response and molecular outliers that arise posttreatment provides new insight into potential early markers of resistance. *Clin Cancer Res; 23(22); 6802–11. ©2017 AACR.*

[1]Division of Medical Oncology, Department of Medicine, Weill Medical College of Cornell University, New York, New York. [2]Vancouver Prostate Centre and Department of Urologic Sciences, University of British Columbia, Vancouver, British Columbia, Canada. [3]Institute of Biosciences and Medical Technology, University of Tampere, Tampere, Finland. [4]Department of Urology, Memorial Sloan Kettering Cancer Center, New York, New York. [5]Department of Medical Oncology, Memorial Sloan Kettering Cancer Center, New York, New York. [6]Department of Medical Oncology, Dana-Farber/Partners Cancer Care, Boston, Massachusetts. [7]Department of Pathology and Laboratory Medicine, Weill Medical College of Cornell University, New York, New York. [8]Institute for Computational Biomedicine, Weill Medical College of Cornell University, New York, New York. [9]Alliance Statistics and Data Center and Department of Biostatistics and Bioinformatics, Duke University, Durham, North Carolina.

Note: Supplementary data for this article are available at Clinical Cancer Research Online (http://clincancerres.aacrjournals.org/).

H. Beltran and A.W. Wyatt contributed equally to this article.

Corresponding Authors: Himisha Beltran, Weill Cornell Medicine, 525 East 68th Street, Box 403, New York, NY 10021. Phone: 646-962-2072; Fax: 646-962-1603; E-mail: hip9004@med.cornell.edu; and Martin E. Gleave, University of British Columbia, Level 6, 2775 Laurel Street. Vancouver, British Columbia V5Z 1M9, Canada. Phone: 604-875-5006; E-mail: m.gleave@ubc.ca

doi: 10.1158/1078-0432.CCR-17-1034

©2017 American Association for Cancer Research.

Introduction

Prostate cancer arises as an androgen-driven disease, dependent on ligand-activation of the androgen receptor (AR) for growth and maintenance (1). Consequently, systemic therapies for advanced prostate cancer have focused on inhibition of AR signaling through reduction of available ligand via androgen deprivation therapy (ADT) or direct antagonism of the AR receptor (2). Even taxane chemotherapies, such as docetaxel, are thought to be effective at least in part through mechanisms that lead to disruption of AR signaling (3, 4). Recent randomized phase III trials have shown that combining docetaxel with ADT for patients with newly diagnosed metastatic hormone-sensitive prostate cancer provides a significant overall survival benefit when compared with ADT monotherapy (5–7).

A rational next question is whether the same benefit may be observed if these therapies were applied earlier in the disease. The multicenter phase III Cancer and Leukemia Group B (CALGB) 90203 trial, "A Randomized Phase III Study of Neo-Adjuvant Docetaxel and Androgen Deprivation Prior to Radical Prostatectomy Versus Immediate Radical Prostatectomy in Patients with High-Risk, Clinically Localized Prostate Cancer," was designed to evaluate this question by studying ADT plus docetaxel in patients

AACR

Translational Relevance

Recent phase III trials have positioned chemohormonal therapy [docetaxel and androgen deprivation therapy (ADT)] as a standard treatment option for patients with advanced hormone-naïve prostate cancer. There are no available molecular biomarkers to identify which patients are most likely to benefit and limited data exploring early mechanisms of treatment resistance. In this study, we demonstrate the feasibility of molecular analyses of pretreatment diagnostic biopsies and posttreated prostatectomy specimens from patients enrolled on a phase III trial of neoadjuvant docetaxel and ADT. Through a multilevel combination of pathology, DNA sequencing, and transcriptome profiling, we offer insights into the acute molecular response to chemohormonal therapy and potential strategies to identify predictive biomarkers.

with newly diagnosed high-risk clinically localized prostate cancer in the neoadjuvant setting. The primary clinical endpoint is to determine whether neoadjuvant therapy decreases 3-year recurrence rates when compared with radical prostatectomy (RP) alone. Patient accrual completed in 2015 and the trial results are expected to be reported in 2018. CALGB is now part of the Alliance for Clinical Trials in Oncology.

Tissue specimens collected from the CALGB 90203 study provide an unprecedented opportunity to understand treatment response and early mechanisms of treatment resistance. This may ultimately elucidate biomarkers to help identify patients most likely to benefit from the combination of ADT and docetaxel. Regardless of the outcome of the CALGB 90203 trial primary endpoint, this biomarker information may also be relevant for the significant proportion of prostate cancer patients with metastatic disease now being treated with standard of care chemohormonal therapy and may ultimately help improve patient selection. Molecular biomarker development for this population will require the development of tools amenable to small amounts of tissue from formalin fixed diagnostic tissue biopsies.

In this proof-of principle study, we posited that resistant pathways observed in metastatic castration-resistant prostate cancer (CRPC) may be detected early in a subset of patients treated with short-term docetaxel and ADT and this is associated with the presence of treatment-resistant cells. Recent metastatic tissue–based studies combined with preclinical modeling have illuminated diverse mechanisms of resistance to AR-directed therapies (8–10) and to docetaxel in the CRPC setting (11–15). Tissue analyses from patients with intermediate and high-risk prostate cancer enrolled in prior phase II trials of neoadjuvant ADT with or without potent AR pathway inhibitors have elucidated changes in AR signaling and correlated the presence of intraprostatic tumor androgens and treatment-induced adaptive response pathway changes with residual disease [e.g., including pathologic complete remission (pCR) and near pCR rates; refs. 16–19]. We previously reported in the CUOG-PO1a trial that two of 64 patients treated with neoadjuvant docetaxel plus androgen ablation for 24 weeks had a complete pathologic response (no tumor in final pathologic specimen; ref. 20). Although complete eradication of cancer following neoadjuvant therapy is rare, path-

ologic specimens often have marked tumor regression that creates challenges in molecular characterization of small residual foci of cancer.

We aimed to develop molecular tools amenable to small amounts of tissue to dissect the genomic and transcriptomic landscape of tumors before and after therapy from patients enrolled on CALGB 90203. We hypothesized that (i) the combination of AR-targeted therapy and docetaxel shapes changes in the molecular landscape of early, aggressive prostate cancer; and (ii) that tumor clones present after therapy may represent either intrinsic or early acquired resistance.

## Materials and Methods

Clinical cohort

Patients with newly diagnosed high-risk, clinically localized prostate adenocarcinoma were enrolled on the phase III CALGB 90203 (Alliance) trial from 2006 to 2015 across the United States and Canada (Fig. 1A). Entry criteria and summary of trial endpoints are described in Supplementary Information. Patients in trial arm A received six cycles of docetaxel at a dose of 75 mg/m^2 administered every 3 weeks in combination with a luteinizing hormone-releasing hormone (LHRH) agonist for 18–24 weeks, followed by RP. Arm B consisted of patients undergoing standard RP without neoadjuvant chemohormonal therapy. A total of 788 patients were enrolled. The primary endpoint is 3-year biochemical PFS and is expected to be completed in 2018. For this study, baseline clinical data, baseline needle biopsies, and RP specimens from 52 of these patients (28 on arm A; 24 on arm B) enrolled at one high volume center [University of British Columbia (UBC)-Vancouver General Hospital] were evaluated (with approval from the UBC Ethics Board and the Alliance Genitourinary Committee). Clinical data and pathology were retrieved locally without access to Alliance central database or biorepository. Each participant signed an Institutional review board-approved, protocol-specific informed consent in accordance with federal and institutional guidelines.

Pathologic evaluation

Formalin-fixed paraffin embedded (FFPE) diagnostic core biopsies and fresh frozen (FF) and FFPE tissue blocks from RP specimens were reviewed by the study pathologist (L. Fazli) for tumor size, Gleason grade, and other morphologic features. Samples were excluded from analysis if insufficient tumor was present due to low cellularity or unavailability of tumor blocks. Overall treatment effect was scored as 0–3 defined by the severity of six morphologic characteristics (Supplementary Methods; Fig. 1B; refs. 21, 22). Representative tumor dense areas and adjacent benign tissue were selected for macrodissection and DNA/RNA extraction (Supplementary Methods).

DNA sequencing

We used targeted sequencing of FFPE needle biopsies and RP specimens using a custom NimbleGen SeqCap EZ Choice Library and Illumina machines. Our custom design includes 72 prostate cancer relevant genes, including AR pathway genes (e.g. *AR*, *FOXA1*, *TMPRSS2*) and other common prostate cancer alterations including *TP53*, *SPOP*, cell-cycle genes (e.g., *CCND1*, *RB1*), DNA repair genes (e.g., *BRCA1/2*, *FANC* family genes, *ATM*, *MSH2/6*), and PI3K pathway genes (e.g., *PIK3CA*, *PTEN*; Supplementary Table S1). Details regarding DNA extraction and sequencing are described in the Supplementary Methods.
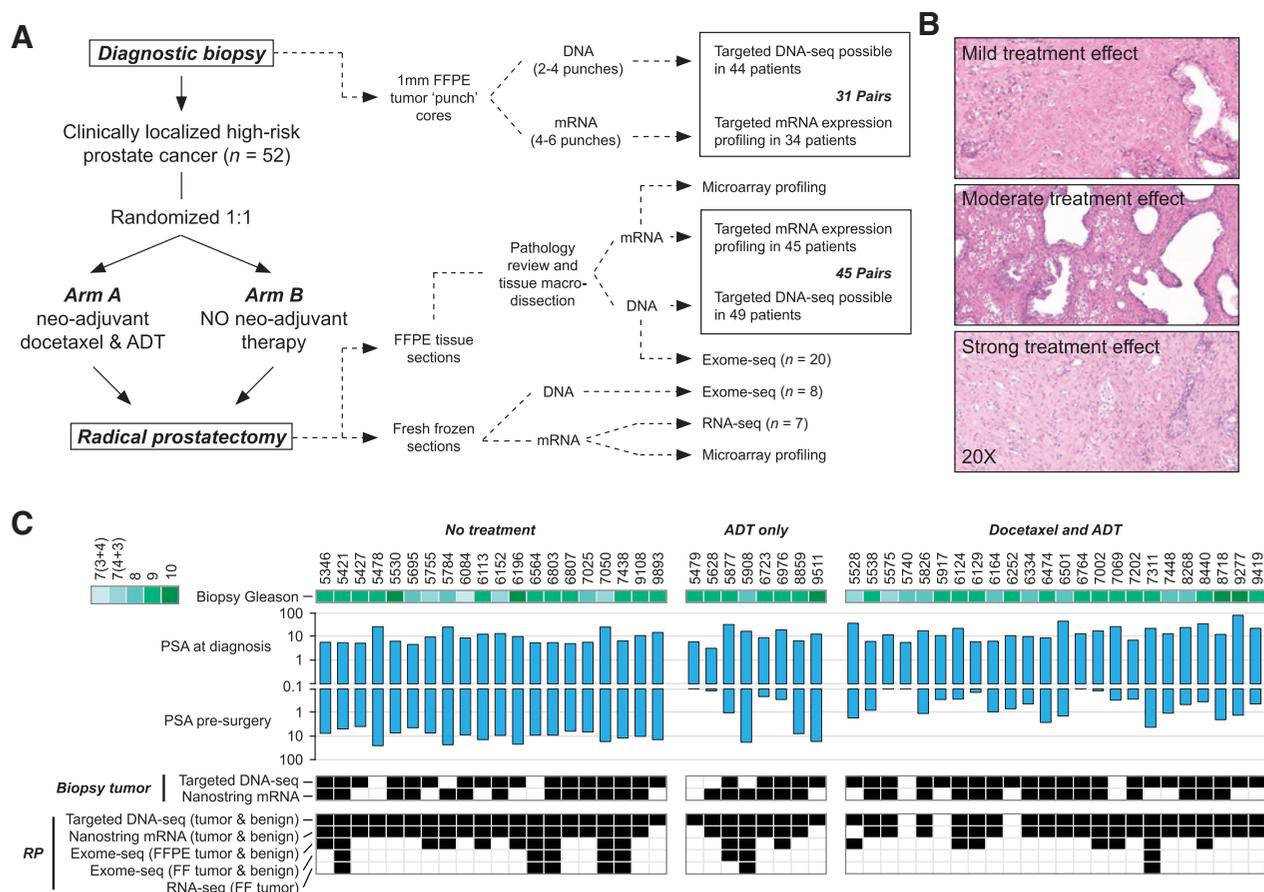
Figure 1.
Study overview. **A,** Schematic illustrating clinical trial design and the nature and number of tissue specimens available for downstream analysis. **B,** Example photomicrographs of H&E-stained RP specimens from the treatment arm demonstrating differing degrees of treatment score. See also Supplementary Fig. S1. **C,** Schematic showing the breakdown of genomic and transcriptomic profiling techniques applied to each patient in the cohort. The effect of treatment on serum prostate-specific antigen (PSA) levels is also provided.

Somatic mutations were identified by comparing allele read counts between tumor and adjacent benign samples. We required somatic mutations to be supported by at least 10 "mutant" reads, and to have a mutant allele fraction of at least 2.0%, at least $2\times$ higher than the allele fraction in the paired normal samples, and at least $20\times$ higher than the background error rate at the site. Mutations in low mappability regions of the genome were discarded. Variant effects were predicted using ANNOVAR version 2016-02-01. Each variant's frequency in the KAVIAR, ExAC, and COSMIC databases was annotated using in-house software. All mutation candidates were manually reviewed for indel-related alignment artifacts, homologous regions, high background error rates, and positional bias using the Integrative Genomics Viewer. Two patients lacked a matched benign tissue sample, and were manually reviewed for mutation candidates of potential germline origin.

To call copy number changes, aligned reads were counted in all captured genome regions using bedtools-2.25.0 (23). GC fractions were calculated for all target regions, and Loess regression was applied to bait logratios to correct for GC content bias. All Loess fits were visually validated for soundness. Coverage logratios were calculated between each sample

and a consensus reference representing the median of all normal samples. Log ratios were corrected for sample-specific differences in overall coverage using median-of-ratios normalization across target regions in chromosomes 2, 4, 12, 14, 15, 19, and 20 (selected for their low rate of copy number alterations in late-stage prostate cancer). All paired normal samples were searched for heterozygous germline SNPs with good coverage, and their allele fractions were calculated in the corresponding tumor samples. A median heterozygous SNP allele fraction $0.5 + $ median $[abs(AF - 0.5)]$ was calculated for every gene in each tumor sample.

Gene expression profiling

We developed a targeted gene panel for this study using the NanoString nCounter that was applied to FFPE biopsy and RP tissues with limited RNA input requirement (<300 ng). The custom gene panel included 163 genes chosen based on their known or potential role in prostate cancer progression, including AR and AR signaling genes (24), the AR V7 splice variant, EMT/plasticity, and neuroendocrine prostate cancer–associated genes (10), cell cycle, WNT, PI3K/AKT pathway genes, TMPRSS2-ERG fusion transcript, and control and housekeeper genes

(Supplementary Table S2). An AR signaling score was quantified for each case using AR pathway genes (24) and methodologies described previously (10) based on correlation with the LNCaP cell line as a reference sample known to have active AR signaling. Details regarding RNA extraction and processing are described in the Supplementary Methods.

Raw count data were normalized using the nSolver analysis software version 2.0, which normalizes samples according to positive and negative control probes and the geometric mean of the six housekeeping primers. RNA from fresh/frozen specimens was also used when available for quality control (QC) and comparative analysis and for RNA-seq when feasible (using protocols previously described; ref. 10). The edgeR package was used to determine genes that were differentially expressed when comparing the treated and untreated cases. To take advantage of the platform design, which includes negative, positive, and housekeeping controls, the normalized counts were used as input measurements for the edgeR library. The negative binomial method was used to identify differentially expressed genes between the treated and untreated cases. The differentially expressed genes were identified by fitting a generalized linear model on the set of 45 RPs, comparing specimens between the two arms. Hierarchical clustering and principal component analysis (PCA) with coefficient of variation (BCV) in edgeR library package distance was used.

Results

Baseline clinical and pathologic features

Baseline clinical characteristics for the 52 patients evaluated in this study are summarized in Table 1 and Supplementary Table S3. Median baseline serum PSA was 11 ng/mL (range 6.3–19.8 ng/mL) and 88% of patients had a Gleason score $\geq$8, reflective of high-risk disease and consistent with the trial eligibility criteria. There were 20 of 52 patients who received no treatment prior to surgery, and 24 of 52 who received combined docetaxel plus ADT (Table 1 and Fig. 1C). A further 8 of 52 received ADT alone due to patients in the treatment arm ($n = 4$) declining chemotherapy or withdrawing after randomization, and patients in the nontreatment arm ($n = 4$) receiving 1–3 months of neoadjuvant ADT (allowed as part of the protocol). Patients receiving docetaxel plus ADT had a higher serum PSA at diagnosis compared with those receiving no treatment (median PSA 13 ng/mL vs. 7.6 ng/mL). However, as expected, presurgery median PSA levels decreased in the docetaxel plus ADT group (0.4 ng/mL vs. 9.1 ng/ml), consistent with biochemical response to therapy.

Table 1. Summary of clinical characteristics

Characteristic	All patients	DOC and ADT	ADT only	No treatment
Number	52	24	8	20
Median age at diagnosis (IQR)	60 (54.5–63.0)	61 (56.8–64.5)	61.5 (58.5–63.3)	56 (52–61)
Median PSA at diagnosis (IQR)	11 (6.3–19.8)	13 (9.6–22.7)	10.8 (6.4–17.3)	7.6 (5.5–12.7)
Biopsy Gleason score				
7	6 (11.5%)	1 (4.2%)	0	5 (25%)
8	12 (23.1%)	8 (33.3%)	1 (12.5%)	3 (15%)
9	30 (57.7%)	13 (54.2%)	7 (87.5%)	10 (50%)
10	4 (7.7%)	2 (8.3%)	0	2 (10%)
Biopsy ISUP score				
2	2 (3.8%)	0	0	2 (10%)
3	3 (5.8%)	1 (4.2%)	0	2 (10%)
4	13 (25.0%)	8 (33.3%)	1 (12.5%)	4 (20%)
5	34 (65.4%)	15 (62.5%)	7 (87.5%)	12 (60)
Median positive cores (IQR)	6 (4–7)	5 (4–6)	7 (5–8)	6 (5–7)
Median PSA presurgery (IQR)	1.85 (0.34–8.82)	0.4 (0.3–1.2)	0.7 (0.2–10.1)	9.1 (7.1–14)
Prostatectomy Gleason score				
7	7 (13%)	3 (13%)	0	4 (20%)
8	2 (4%)	0	1 (12.5%)	1 (5%)
9	23 (44%)	5 (21%)	5 (62.5%)	13 (65%)
10	3 (6%)	1 (4%)	0	2 (10%)
Unknown (artifact)	17 (33%)	15 (62%)	2 (25%)	0
Prostatectomy ISUP score				
2	3 (5.8%)	2 (8.3%)	0	1 (5%)
3	3 (5.8%)	1(4.2%)	0	2 (10%)
4	3 (5.8%)	0	1 (12.5%)	2 (10%)
5	26 (50.0%)	6 (25%)	5 (62.5%)	15 (75%)
Unknown (artifact)	17 (32.6%)	15 (62.5%)	2 (25%)	0
Final pathologic stage				
T2a	3 (6%)	2 (8.3%)	1 (12.5%)	0
T2b	1 (2%)	1 (4.2%)	0	0
T2c	8 (15%)	5 (20.8%)	0	3 (15%)
T3a	18 (35%)	8 (33.3%)	2 (25%)	8 (40%)
T3b	19 (36%)	7 (29.1%)	5 (62.5%)	7 (35%)
T4	3 (6%)	1 (4.2%)	0	2 (10%)
Postoperative margin status				
Positive	20 (38%)	6 (25%)	3 (37.5%)	9 (45%)
Negative	32 (62%)	18 (75%)	5 (62.5%)	11 (55%)
Lymph node involvement				
Positive	11 (21%)	5 (21%)	2 (25%)	4 (20%)
Negative	41 (79%)	19 (79%)	6 (75%)	16 (80%)

Abbreviations: DOC, docetaxel; IQR, interquartile range. Also see Supplementary Table S1.

Representative photomicrographs of pathology review on tumor cellularity and treatment effect are shown in Fig. 1B and Supplementary Fig. S1. There were 49 of 52 RPs (94%) with sufficient tumor and matched normal material for DNA extraction (3/52 had near complete pathologic responses), which was successful in all 49 cases (median yield = 1,450 ng). Of these, mRNA was successfully extracted and met quality control standards for NanoString in 45 cases (median 265 ng RNA).

Although 58% of patients had their diagnostic biopsies (prior to study enrollment) performed outside Vancouver General Hospital, we were able to obtain FFPE biopsy blocks for 49 of 52 patients. On the basis of pathology review, 47 of 49 (96%) of diagnostic biopsies had sufficient tumor material for DNA and RNA extraction. DNA extraction was successful in 44 of 47, with a median yield of 28 ng. Thirty-four needle biopsies met QC standards for NanoString analysis (median 255 ng RNA). Analysis of both DNA and RNA of matched biopsy and RP pairs was feasible for 34 of 47 [81%; 95% confidence interval (CI), 67%–91%] patients (Fig. 1A and C).

The dates of subject enrollment ranged between 2006 and 2015. The median age of tumor biopsy tissue specimens at time of molecular analysis for this study was 66 months (range 7–97 months) and the median age of RP specimens was 61 months (range 5–86 months).

Differences in mutational landscape before and after neoadjuvant treatment

We performed targeted DNA sequencing across a panel of 72 known prostate cancer genes (Supplementary Table S1). Median on-target sequencing depth in the RP specimens was approximately 500×. Predictably, the archival biopsy specimens gave more variable data including a high frequency of PCR duplicates and reduced target region coverage (Supplementary Fig. S2). Although this variability did not affect mutation calling, there were inherent biases in copy number profiles that were not explained by GC fraction of target regions, extracted DNA yield, or systematic differences between biopsy and prostatectomy

samples. Therefore, we excluded biopsy copy number calls from global analyses.

Forty-two of 52 (81%) patients had DNA sequencing performed on paired biopsy and RP specimens, with 9 of the remaining 10 patients having either biopsy or RP data alone. Minimum tumor cell fractions from targeted DNA sequencing are reported in Supplementary Table S5. Across the cohort, we detected a total of 106 somatic mutations, including 57 predicted to cause coding changes (18 were truncating mutations; Supplementary Table S5). Coding somatic mutations were consistent with aggressive primary prostate cancer (25), including deleterious mutations involving FOXA1 ($n = 6$), SPOP ($n = 4$), PTEN ($n = 6$), and KMT2C ($n = 6$; Fig. 2; Supplementary Fig. S3). Eleven patients (22%) had pathogenic mutations in TP53 [compared with TCGA frequency of 59 of 498 (12%)]. Three of 52 patients harbored truncating germline mutations involving DNA damage repair genes BRCA2 ($n = 2$) or ATM (Supplementary Table S6). Whole-exome sequencing of adjacent FFPE sections and/or fresh/frozen tissue blocks from 20 RP cases confirmed mutation calls from targeted sequencing and did not reveal any additional mutations across the 72 genes in our panel (Supplementary Table S7).

Among the diagnostic biopsies evaluated, 35 of 44 (80%) had ≥1 somatic mutation, with 23 of 44 (52%) having ≥1 nonsynonymous mutation (Fig. 2; Supplementary Fig. S3). This is consistent with recent TCGA data where 159 of 333 (48%) of primary prostate cancer had ≥1 nonsynonymous mutation in the 72 genes across our panel (25). Although 85% of the pretreatment biopsies from patients receiving subsequent neoadjuvant therapy had mutations, after treatment (i.e., in RP specimens) this figure was 59% (in untreated patients this comparison was 75% vs. 71%). The average number of detected somatic mutations was not lower in treated compared with untreated RP specimens (1.0 vs. 1.55; Supplementary Fig. S4). Average mutant/variant allele frequency (MAF) was significantly lower in posttreated RP specimens (mean = 13.4%) compared with either pretreatment biopsy (mean = 24.1%; t test) or untreated RP specimens (mean = 24.7%; Supplementary Fig. S4). This trend was particularly
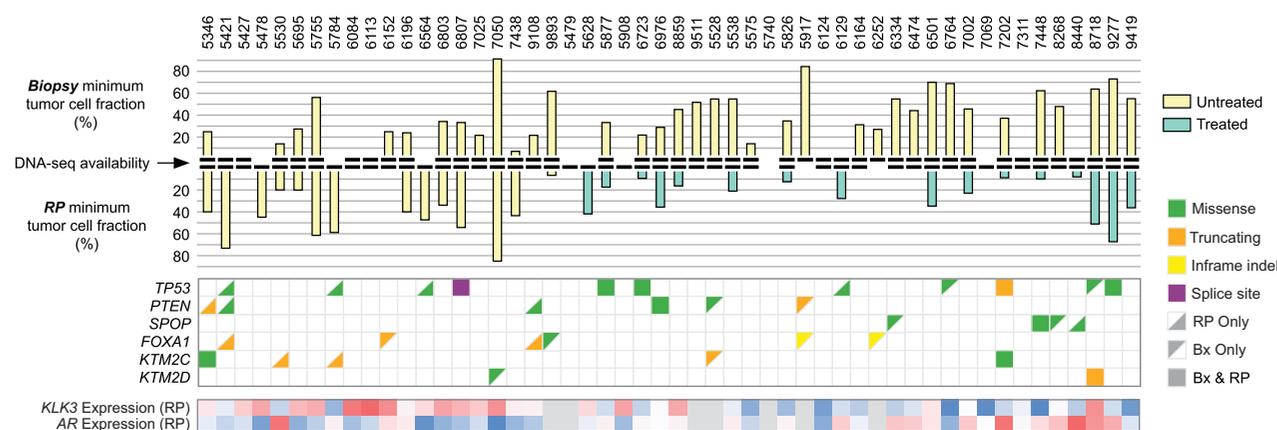
Figure 2.
Somatic mutations detected in diagnostic biopsy cores and matched RP specimens. The bar plot shows minimum tumor cellularity predicted from targeted DNA sequencing of 72 prostate cancer driver genes in biopsy (top) and RP (bottom). For some specimens, no somatic mutations were detected within the target regions meaning that tumor cellularity was unknown (indicated by lack of yellow or green bars). Mutations in frequently altered genes are provided in an oncoprint (also see Supplementary Fig. S3). The bottom plot is a heatmap highlighting persistent AR expression in posttreated specimens (seven patients did not have expression data available and are indicated with filled gray boxes).

evident among paired mutations (i.e., those shared by matched biopsy and RP), where 95% of mutations in posttreatment RP specimens had a lower MAF than in the matched pretreatment biopsy, compared with only 33% in the untreated specimens [mean (median) fold change treated vs. untreated: 0.47 (0.40) vs. 2.02 (1.13); Supplementary Fig. S4]. Overall, these data are consistent with a variable reduction in tumor cellularity/burden posttreatment and raises the possibility of reduced tumor clone diversity in the wake of potent chemohormonal therapy. Despite this decrease in mutational detection posttherapy, there were significant tumor cell–intrinsic gene expression changes detected across the cohort as described below.

Recent metastatic tissue biopsy studies have suggested that some gene mutations are enriched in CRPC compared with primary treatment–naïve prostate cancer. For example, TP53 mutations are found in 46.7% of CRPC but only 12.2% of primary tumors, whereas mutations in the AR ligand–binding domain are present in 20% –25% of CRPC but absent from untreated prostate cancer (8, 25). The latter are a mechanism by which prostate cancer cells become resistant to ADT. Among the RP specimens exposed to neoadjuvant therapy, individual gene mutation frequencies were not high enough to detect a statistically significant trend posttreatment (e.g., consistent enrichment or depletion). However, five TP53 mutations were detected in the posttreated specimens (Supplementary Fig. S5). Two patients with pathogenic FOXA1 mutations in their pretreatment biopsy had an apparent pathologic complete response in the RP specimen (and no tissue available for sequencing). We did not detect any AR mutations in posttreated RPs (at >1% MAF), suggesting that 4.5 months of ADT is not sufficient time to yield a large population of AR-mutant clones.

Copy number alterations in the untreated RP specimens were consistent with high-risk disease, including frequent PTEN (8/22) and RB1 (6/22) loss (examples in Supplementary Fig. S6). However, there were some unusual events including a deep deletion of ZBTB16 in the biopsy and RP specimen from one patient (case 5346), and an amplification of CDK6 in both the biopsy and RP specimen from another patient (case 6803; Supplementary Fig. S6). Homozygous deletions of the transcriptional repressor and putative tumor suppressor ZBTB16 (PLZF) were recently identified in CRPC (8, 26).

Evidence of treatment-induced transcriptome changes

Gene expression levels of the panel of 163 genes and a list of differentially expressed genes by univariate analysis are summarized in Supplementary Tables S8–S11. For seven RP specimens with sufficient fresh/frozen tissue for both NanoString and RNA-seq, gene expression was compared and showed high correlation (average Pearson correlation coefficient = 0.85; Supplementary Fig. S7); NanoString from matched FFPE and fresh/frozen tissue were also compared and showed high correlation (Pearson correlation coefficient = 0.96; Supplementary Fig. S8). Copy number losses, such as PTEN (detected by DNA sequencing), were associated with lower expression at the mRNA level (Supplementary Fig. S9). TMPRSS2-ERG fusion transcript was detected in 32 cases and associated with ERG mRNA overexpression (Pearson correlation coefficient = 0.8; Supplementary Fig. S10).

Unsupervised analysis of mRNA data of RP specimens of all the genes revealed clustering of treated and untreated cases (Supplementary Figs. S11–S13). Differentially expressed genes are depicted in Fig. 3 and reported in Supplementary Table S8.

Molecularly distinct subsets were identified in both groups and were not explained by differences in tumor cellularity (Supplementary Fig. S13). When comparing tumors with high minimum tumor cellularity to those with low (or unknown) tumor cellularity from targeted DNA sequencing, we also did not observe large differences in the levels of relatively tumor cell–intrinsic mRNA transcripts such as AR, KLK3, or ERG (Supplementary Fig. S14). The heterogeneity observed is supportive of a likely lack or minimal contribution of batch effect or poor signal driving changes and likely driven by biologic differences among patients. In the neoadjuvant treatment arm, the majority of the evaluated genes were significantly upregulated compared with untreated RP cancers (Supplementary Table S8 and Supplementary Fig. S12).

As expected, there was significant downregulation of the AR target gene KLK3 (PSA) expression in posttreated RP specimens concordant with an overall decline in serum PSA (Fig. 4; Supplementary Fig. S15), although the degree of suppression of AR signaling genes and AR score in treated cases varied (Supplementary Figs. S16–S17). Expression of both AR and AR-V7 transcripts were higher in the treated group (Fig. 4) and strongly correlated; the ratio of AR-V7 to wild-type AR was similar to the untreated cases (Supplementary Fig. S18). Although baseline PSA was higher in the treated subgroup, there were no significant differences in baseline biopsy tissue PSA (KLK3) expression to explain differences in posttreatment AR signaling (Supplementary Figs. S19–S20). We also observed significant upregulation of other hormone receptors [i.e., estrogen receptor (ESR1), progesterone receptor (NRC3C), glucocorticoid receptor (NRC31)] in posttreated specimens (Fig. 3). These observations are potentially explained by residual AR activity and/or activity of alternative transcriptional activators (i.e., AR bypass mechanisms).

There was higher gene expression of a subset of plasticity and neuroendocrine lineage genes in posttreated specimens including classical neuroendocrine markers such as chromogranin A (CHGA; Supplementary Fig. S21). Paternally Expressed 10 (PEG10), a retrotransposon-derived gene upregulated during neuroendocrine trans-differentiation and functionally linked to Rb and p53 (27), was also higher in treated cases (Supplementary Fig. S22). The SPDEF gene, recently found to be downregulated in metastatic castration-resistant neuroendocrine prostate cancer due to DNA methylation (10) was also significant downregulated in the treated versus untreated specimens from this cohort (Supplementary Fig. S23). SPDEF is an ETS family transcription factor, previously described as a regulator of cellular differentiation and suppressor of tumor metastasis through inhibition of epithelial-to-mesenchymal transition (EMT; ref. 28). Treatment-induced upregulation of neuroendocrine markers including PEG10 and downregulation of SPDEF are hypothesis generating and suggest that plasticity may occur after short-term therapy. The frequency and prognostic value of these markers and their relationship with other lineage plasticity–associated genomic alterations such as TP53 and RB1 (29–31) and MYCN (32, 33) will be elucidated with more cases and extended follow-up.

Surprisingly, there was one significant outlier case in the untreated arm with very high neuroendocrine marker expression (Fig. 3). These findings prompted re-review of the pathology for this case, and the tumor was confirmed by morphology to be a high-grade neuroendocrine carcinoma (Supplementary Fig. S24) with diffusely positive staining for neuroendocrine markers by IHC. These findings highlight the capability of the platform in
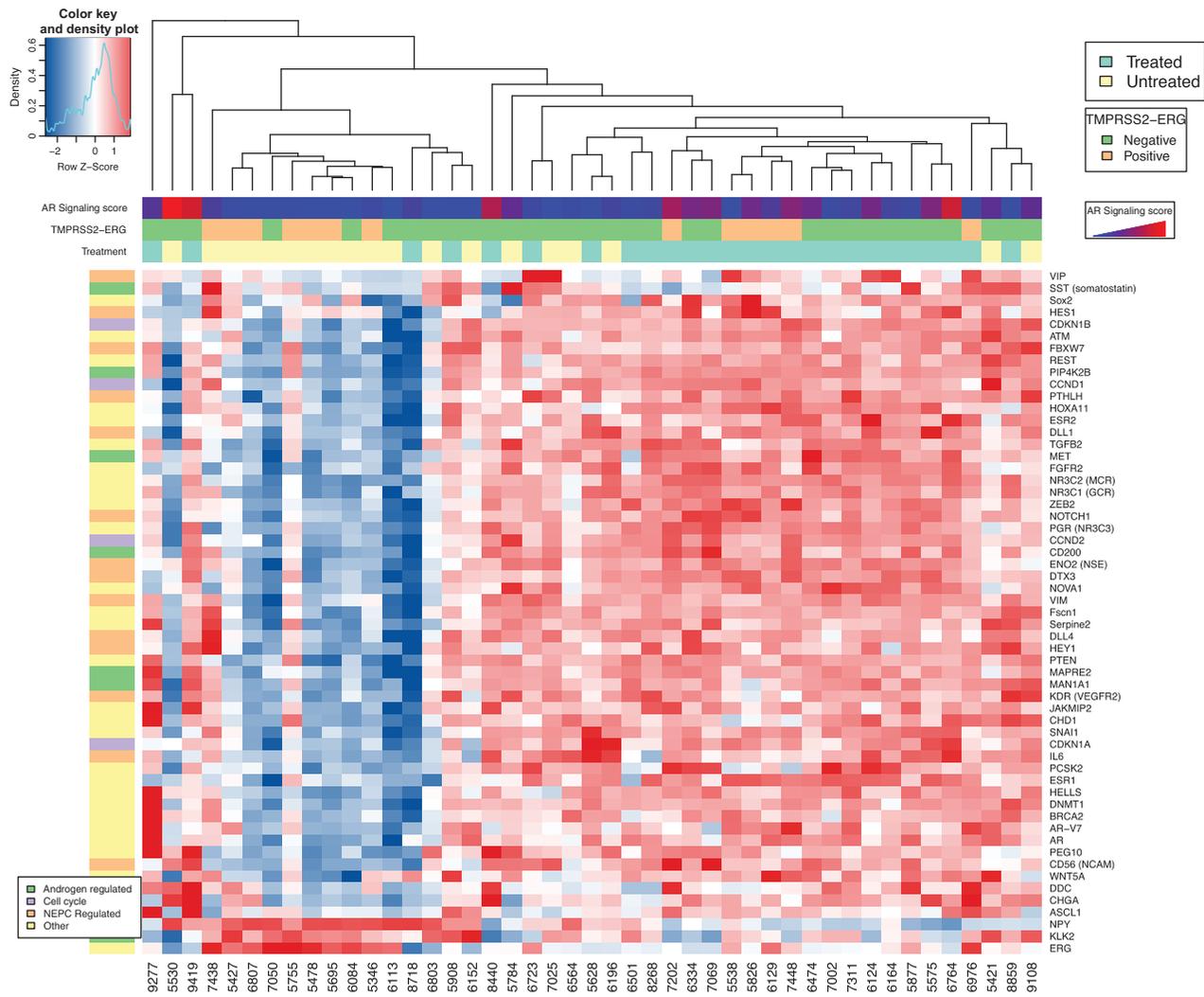
Figure 3.
Differentially expressed genes between treated and untreated patient subgroups. Differentially expressed genes ($n = 57$) were calculated on the basis of a t test with corrected P values < 0.15 (Benjamini–Hochberg method). Red, high expression; blue, low expression. Gene categories are highlighted and AR signaling score (red = high, blue = low), TMPRSS2-ERG fusion transcript (green = negative, orange = positive), and treatment status (yellow-untreated or blue = treated arm) are annotated.

identifying histologic variants based on molecular features and support the evaluation of pretreatment biopsies in neoadjuvant studies for the presence of preexisting changes. We therefore also compared patient-matched prostate needle biopsies with prostatectomy samples in individual patients ($n = 34$). As expected, the pretreatment biopsies and posttreated specimens showed significant clustering in the treated arm (Supplementary Fig. S25) with no significant differences observed in the untreated arm (Supplementary Fig. S26). Relative fold changes in gene expression and differentially expressed genes between patient matched pretreated and posttreated specimens are shown in Supplementary Figs. S27 and S28, which demonstrated heterogeneity in the degree of upregulation of neuroendocrine markers and downregulation of AR target genes including the TMPRSS2-ERG fusion transcript (Supplementary Figs. S29 and S30). Notably, the degree of suppression of AR target genes such as PSA (KLK3), NXK3.1, and TMPRSS2 between matched needle biopsies and neoadjuvantly

treated RP specimens significantly correlated with the degree of serum PSA decline in patients before and after neoadjuvant therapy (e.g., Pearson $R = 0.36$ for KLK3; $R = 0.43$ for TMPRSS2), in contrast to a negligible correlation observed between biopsies and RP specimens in untreated patients (Fig. 4B; Supplementary Fig. S31).

Integrative analysis of outlier cases

RP specimens of two patients (9277 and 8718) that received combined chemohormonal therapy showed less evidence of therapy effect than the rest of the cohort. Both cases had Gleason score 10 at diagnosis, and after neoadjuvant therapy both had nadir presurgery serum PSA levels >1 ng/mL as well as significant residual disease by pathology with high Ki67 proliferative index (Supplementary Fig. S32). Unlike other treated cases, there was no difference in mutation allele frequency between the pretreatment biopsy and posttreatment RP specimens (Fig. 2). Case 9277 had a
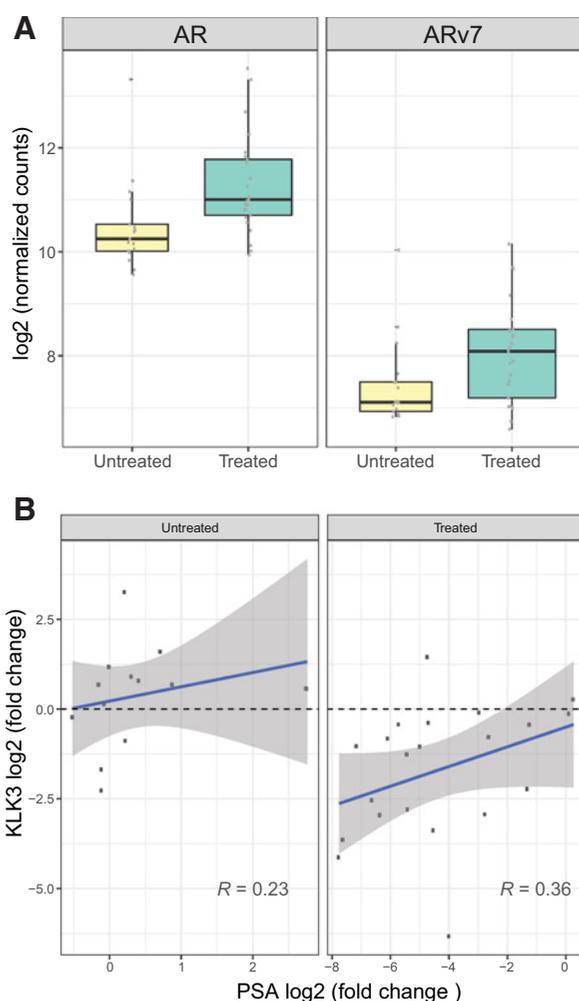
Figure 4.
Differences in the expression of the AR, AR-variant 7, and PSA between treated and untreated subgroups. **A,** AR and AR-V7 gene expression in untreated and treated specimens. **B,** Change of tissue PSA expression (KLK3) versus change in serum PSA levels in untreated and treated patients. R, Pearson correlation.

genomic landscape more consistent with advanced prostate cancer, including *TP53* mutation, biallelic *APC* mutation, and *PTEN*, *CDKN1B*, and *RB1* copy number loss (Supplementary Fig. S32). Notably, there was also evidence of a copy number gain at the *AR* locus (not present in the pretreatment biopsy from 9277), and the posttreated specimen of this case had among the highest AR expression compared with the rest of the cohort. Furthermore, gene expression clustering also demonstrated that this case was a unique outlier (Fig. 3). When comparing baseline pretreatment and posttreated specimens for case 8718, AR mRNA expression was high at baseline and increased over 2-fold after therapy. Furthermore, based on expression profiles, 8718 clustered closer to the untreated specimens rather than the bulk of the treated tumors (Fig. 3). Conversely in a third case (5917), also a patient with a high-grade tumor (Gleason 9) at diagnosis, and high VAF mutations involving *PTEN* and *FOXA1* in his pretreatment biopsy, he had a complete pathologic response in his RP specimen such that no tumor tissue was available for macrodissection.

Discussion

The CALGB 90203 study is a multi-institutional phase III clinical trial designed to evaluate the clinical benefit of neoadjuvant docetaxel in combination with ADT for patients with high-risk clinically localized prostate cancer. Residual tumor cells in the prostate after neoadjuvant therapy may possess characteristics representing intrinsic resistance or the early emergence of resistance pathways. Although these resistant cells may likely require additional "hits" to trigger clinical progression, we hypothesized that resistant pathways observed in metastatic CRPC may be detected in a subset of patients treated on CALGB 90203.

Obtaining sufficient quality and quantity of nucleic acids from archival specimens including diagnostic needle biopsy tissue and posttreatment prostatectomy tissue required to test this hypothesis is a considerable challenge. In this study, we established and validated protocols amenable to formalin-fixed tissues to demonstrate the feasibility of obtaining robust targeted exome and transcript data. On the basis of prior studies, we know that AR signaling is reactivated in the majority of CRPC which can occur through activating mutations or amplifications involving the AR gene, expression of AR splice variants (e.g., AR-V7), intratumoral steroidogenesis, or other mechanisms (34, 35). AR mutations and copy number gains, present in 60% of metastatic CRPC tumors, are not observed in untreated primary tumors. To our knowledge, no prior studies have examined how rapidly AR genomic alterations emerge during initial ADT and which primary lesions are most likely to develop AR alterations. The notable paucity of AR mutations or amplifications by deep sequencing of the AR gene in our study suggests that these are typically later events. Although AR-V7 expression increased along with wild-type AR gene expression, the AR-V7/AR-WT ratio remained unchanged in treated specimens. Despite no obvious changes in AR itself, the degree of AR signaling activity and the depth of AR target suppression did vary between patients and were dynamic in patient-matched specimens before and after neoadjuvant therapy, consistent with that observed in prior early-phase neoadjuvant ADT trials (16, 17, 19). Overall, these data suggest that AR signaling is relevant at early time-points and potentially driving response and resistance to therapy, yet is not likely driven through the common mechanisms associated with later AR reactivation in CRPC.

Genomic and transcriptomic alterations in several other signaling pathways, including PI3K/AKT, WNT, and DNA repair are enriched in advanced prostate cancer, and in some cases are capable of driving CRPC progression (8, 36). Because primary treatment-naïve prostate cancer is heterogeneous and often multifocal within a single patient (37–40), whenever feasible, we analyzed spatially distinct macrodissected tumors. As expected, we observed commonly reported prostate cancer genomic alterations (e.g., *SPOP* math domain missense mutations, *PTEN* loss) as well as alterations associated with poor prognosis disease (e.g., loss of function alterations involving *TP53* and *RB1*), consistent with the high-risk cases enrolled in this trial. Three of the 52 patients harbored pathogenic germline DNA repair gene mutations, recently reported in up to 12% of metastatic prostate cancer (41), but with an unclear etiologic role in high-risk disease. Targeted sequencing indicated an overall reduction in tumor cellularity induced by treatment, but with marked variability between patients. Low tumor cellularity at prostatectomy, despite an initial diagnosis of high volume high-grade disease (by biopsy), may be an indicator of

therapy response and should be explored in the final trial analyses. In some patients, high volume residual disease remained and was marked by high allele frequency mutations and distinct transcript profiles, suggesting enduring fitness of certain clones. It is plausible that neoadjuvant therapy shapes the clonal architecture and this hypothesis can be explored with more CALGB 90203 cases and clinical follow-up. Furthermore, the incidence and clinical impact of germline alterations involving DNA repair genes in this expanded high-risk clinically localized prostate cancer cohort will be elucidated.

In a subset of CRPC, loss of AR signaling dependence can occur and this is often associated with lineage plasticity, activation of distinct transcriptional and epigenetic neuroendocrine-lineage pathways, and/or genomic alterations involving RB1, TP53, and MYCN (10, 29–31, 42). Although most studies looking at lineage plasticity and the neuroendocrine phenotype have focused on CRPC, in this study we identified cases in which changes in these pathways could be detected early in a subset of patients treated with neoadjuvant therapy. This may represent an early adaptive response or possibly early acquired resistance. Evaluation of pretreatment biopsies was needed to elucidate preexisting changes from those that were treatment induced. There is likely variability of AR dependence in individual patients with high-risk localized prostate adenocarcinoma and early neuroendocrine reprogramming and epithelial plasticity may start to emerge in outliers even in the context of short-term therapy, a framework further supported by our previously reported dynamic patient-derived xenograft (PDX) model (27, 43) derived from a similar AR-positive, PSA-positive untreated tumor from a high-risk clinically localized prostate cancer patient. The tumor, which was TP53 and RB1 null, developed neuroendocrine prostate cancer upon PDX castration with retention of genomic alterations from the parent tumor and acquisition of neuroendocrine histologic and gene expression changes including suppressed AR signaling. These CALGB 90203 observations have implications in understanding the acute tumor response to therapy, possibly representing a reversible or "plastic" state, and may inform the development of future prognostic biomarkers.

Preclinical data combined with clinical observations have provided insights into docetaxel resistance and have functionally linked stress chaperones (11–13) as well as the cyclin/CDK/ RB pathway and ERG rearrangement status to taxane resistance (14, 15). Clinical trial data suggest that the AR-V7 variant is not associated with taxane resistance (44, 45). The extended datasets that will be generated by CALGB 90203 coupled with clinical features and outcomes and compared with ongoing contemporary neoadjuvant ADT studies may help dissect the relative contributions of AR versus taxane resistance in the hormone-naïve clinical setting.

In this proof-of-principle study, we demonstrate the feasibility of obtaining robust and reliable genomic and transcript data with small amounts of neoadjuvant treated, archival tissue. We were able to detect, quantify, and verify tumor mutations, AR signaling patterns, AR splice variant expression, and fusion transcripts. Limitations include the minimal tumor present in pretreatment

needle biopsies and posttreated tumors and the methods used for storing archival tissue specimens (as formalin fixed rather than banked fresh/frozen), both of which preclude more extensive molecular analysis. Therefore, integrative analyses are limited to a select panel of genes, and the discovery of new resistance genes or other pathways including the analysis of intratumoral androgens was not picked up through these methods. Furthermore, other readouts of biologic pathway activation including proteomic, metabolomics, and immunologic changes could not be identified using this approach. Primary prostate cancers are commonly multifocal, and paired analyses comparing biopsies and prostate RP specimens may also be confounded by intrapatient heterogeneity. Ongoing efforts are focused on extending the analysis to additional patients in the CALGB 90203 cohort, inclusion of additional genes to the panels, assessment of spatially distinct tumors when feasible, analysis for frequency of germline DNA repair alterations in this high-risk prostate cancer cohort, and clinical correlation with clinical variables and the prespecified endpoints of the trial.

Disclosure of Potential Conflicts of Interest

No potential conflicts of interest were disclosed.

Authors' Contributions

Conception and design: H. Beltran, A.W. Wyatt, J. Eastham, M. Morris, M.-E. Taplin, S. Halabi, M.E. Gleave
Development of methodology: H. Beltran, A.W. Wyatt, E.C. Chedgy, A. Sboner, S. Halabi, M.E. Gleave
Acquisition of data (provided animals, acquired and managed patients, provided facilities, etc.): H. Beltran, E.C. Chedgy, A. Donoghue, E.W. Warner, K. Beja, C.C. Collins, J. Eastham, M.-E. Taplin
Analysis and interpretation of data (e.g., statistical analysis, biostatistics, computational analysis): H. Beltran, A.W. Wyatt, E.C. Chedgy, A. Donoghue, M. Annala, E.W. Warner, M. Sigouros, F. Mo, J. Eastham, M. Morris, M.-E. Taplin, A. Sboner, S. Halabi, M.E. Gleave
Writing, review, and/or revision of the manuscript: H. Beltran, A.W. Wyatt, E.C. Chedgy, E.W. Warner, J. Eastham, M. Morris, M.-E. Taplin, A. Sboner, S. Halabi
Administrative, technical, or material support (i.e., reporting or organizing data, constructing databases): H. Beltran, A. Donoghue, K. Beja, M. Sigouros, C.C. Collins, M. Morris
Study supervision: H. Beltran, A.W. Wyatt, M.-E. Taplin, M.E. Gleave
Other (pathology): L. Fazli
Other (PI of NIH grant): S. Halabi
Other (enrollment of subjects into clinical trial biobanking of radical prostatectomy specimens): M.E. Gleave

Grant Support

References

1. Huggins C, Hodges CV. Studies on prostatic cancer. 1. The effects of castration, of estrogen and androgen injection on serum phosphatases in metastatic carcinoma of the prostate. Cancer Res 1941;1:293–7.

2. Knudsen KE, Scher HI. Starving the addiction: new opportunities for durable suppression of AR signaling in prostate cancer. Clin Cancer Res 2009;15:4792–8.

3. Thadani-Mulero M, Nanus DM, Giannakakou P. Androgen receptor on the move: boarding the microtubule expressway to the nucleus. Cancer Res 2012;72:4611–5.

4. Zhu ML, Horbinski CM, Garzotto M, Qian DZ, Beer TM, Kyprianou N. Tubulin-targeting chemotherapy impairs androgen receptor activity in prostate cancer. Cancer Res 2010;70:7992–8002.

5. James ND, Sydes MR, Clarke NW, Mason MD, Dearnaley DP, Spears MR, et al. Addition of docetaxel, zoledronic acid, or both to first-line long-term hormone therapy in prostate cancer (STAMPEDE): survival results from an adaptive, multiarm, multistage, platform randomised controlled trial. Lancet 2016;387:1163–77.

6. Sweeney CJ, Chen YH, Carducci M, Liu G, Jarrard DF, Eisenberger M, et al. Chemohormonal therapy in metastatic hormone-sensitive prostate cancer. N Eng J Med 2015;373:737–46.

7. Vale CL, Burdett S, Rydzewska LH, Albiges L, Clarke NW, Fisher D, et al. Addition of docetaxel or bisphosphonates to standard of care in men with localised or metastatic, hormone-sensitive prostate cancer: a systematic review and meta-analyses of aggregate data. Lancet Oncol 2016;17:243–56.

8. Robinson D, Van Allen EM, Wu YM, Schultz N, Lonigro RJ, Mosquera JM, et al. Integrative clinical genomics of advanced prostate cancer. Cell 2015;161:1215–28.

9. Grasso CS, Wu YM, Robinson DR, Cao X, Dhanasekaran SM, Khan AP, et al. The mutational landscape of lethal castration-resistant prostate cancer. Nature 2012;487:239–43.

10. Beltran H, Prandi D, Mosquera JM, Benelli M, Puca L, Cyrta J, et al. Divergent clonal evolution of castration-resistant neuroendocrine prostate cancer. Nat Med 2016;22:298–305.

11. Zhang F, Kumano M, Beraldi E, Fazli L, Du C, Moore S, et al. Clusterin facilitates stress-induced lipidation of LC3 and autophagosome biogenesis to enhance cancer cell survival. Nat Commun 2014;5:5775.

12. Zoubeidi A, Gleave M. Small heat shock proteins in cancer therapy and prognosis. Int J Biochem Cell Biol 2012;44:1646–56.

13. Zoubeidi A, Chi K, Gleave M. Targeting the cytoprotective chaperone, clusterin, for treatment of advanced cancer. Clin Cancer Res 2010;16: 1088–93.

14. de Leeuw R, Berman-Booty LD, Schiewer MJ, Ciment SJ, Den RB, Dicker AP, et al. Novel actions of next-generation taxanes benefit advanced stages of prostate cancer. Clin Cancer Res 2015;21:795–807.

15. Galletti G, Matov A, Beltran H, Fontugne J, Miguel Mosquera J, Cheung C, et al. ERG induces taxane resistance in castration-resistant prostate cancer. Nat Commun 2014;5:5548.

16. Taplin ME, Montgomery B, Logothetis CJ, Bubley GJ, Richie JP, Dalkin BL, et al. Intense androgen-deprivation therapy with abiraterone acetate plus leuprolide acetate in patients with localized high-risk prostate cancer: results of a randomized phase II neoadjuvant study. J Clin Oncol 2014;32:3705–15.

17. Mostaghel EA, Nelson PS, Lange P, Lin DW, Taplin ME, Balk S, et al. Targeted androgen pathway suppression in localized prostate cancer: a pilot study. J Clin Oncol 2014;32:229–37.

18. Mostaghel EA, Cho E, Zhang A, Alyamani M, Kaipainen A, Green S, et al. Association of tissue abiraterone levels and SLCO genotype with intraprostatic steroids and pathologic response in men with high-risk localized prostate cancer. Clin Cancer Res 2017;23:4592–601.

19. Montgomery B, Tretiakova MS, Joshua AM, Gleave ME, Fleshner N, Bubley GJ, et al. Neoadjuvant enzalutamide prior to prostatectomy. Clin Cancer Res 2017;23:2169–76.

20. Chi KN, Chin JL, Winquist E, Klotz L, Saad F, Gleave ME. Multicenter phase II study of combined neoadjuvant docetaxel and hormone therapy before radical prostatectomy for patients with high risk localized prostate cancer. J Urol 2008;180:565–70.

21. Bostwick DG, Meiers I. Diagnosis of prostatic carcinoma after therapy - Review 2007. Arch Pathol Lab Med 2007;131:360–71.

22. Efstathiou E, Abrahams NA, Tibbs RF, Wang X, Pettaway CA, Pisters LL, et al. Morphologic characterization of preoperatively treated prostate cancer: toward a post-therapy histologic classification. Eur Urol 2010; 57:1030–8.

23. Quinlan AR, Hall IM. BEDTools: a flexible suite of utilities for comparing genomic features. Bioinformatics 2010;26:841–2.

24. Hieronymus H, Lamb J, Ross KN, Peng XP, Clement C, Rodina A, et al. Gene expression signature-based chemical genomic prediction identifies a novel class of HSP90 pathway modulators. Cancer Cell 2006;10:321–30.

25. Cancer Genome Atlas Research Network. The molecular taxonomy of primary prostate cancer. Cell 2015;163:1011–25.

26. Xiao GQ, Unger P, Yang Q, Kinoshita Y, Singh K, McMahon L, et al. Loss of PLZF expression in prostate cancer by immunohistochemistry correlates with tumor aggressiveness and metastasis. PLoS One 2015;10:e0121318.

27. Akamatsu S, Wyatt AW, Lin D, Lysakowski S, Zhang F, Kim S, et al. The placental gene PEG10 promotes progression of neuroendocrine prostate cancer. Cell Rep 2015;12:922–36.

28. Steffan JJ, Koul S, Meacham RB, Koul HK. The transcription factor SPDEF suppresses prostate tumor metastasis. J Biol Chem 2012;287:29968–78.

29. Mu P, Zhang Z, Benelli M, Karthaus WR, Hoover E, Chen CC, et al. SOX2 promotes lineage plasticity and antiandrogen resistance in TP53- and RB1-deficient prostate cancer. Science 2017;355:84–8.

30. Ku SY, Rosario S, Wang Y, Mu P, Seshadri M, Goodrich ZW, et al. Rb1 and Trp53 cooperate to suppress prostate cancer lineage plasticity, metastasis, and antiandrogen resistance. Science 2017;355:78–83.

31. Zou M, Toivanen R, Mitrofanova A, Floch N, Hayati S, Sun Y, et al. Transdifferentiation as a mechanism of treatment resistance in a mouse model of castration-resistant prostate cancer. Cancer Discov 2017;7: 736–49.

32. Dardenne E, Beltran H, Benelli M, Gayvert K, Berger A, Puca L, et al. N-Myc induces an EZH2-mediated transcriptional program driving neuroendocrine prostate cancer. Cancer Cell 2016;30:563–77.

33. Lee JK, Phillips JW, Smith BA, Park JW, Stoyanova T, McCaffrey EF, et al. N-Myc drives neuroendocrine prostate cancer initiated from human prostate epithelial cells. Cancer Cell 2016;29:536–47.

34. Wyatt AW, Gleave ME. Targeting the adaptive molecular landscape of castration-resistant prostate cancer. EMBO Mol Med 2015;7:878–94.

35. Ferraldeschi R, Welti J, Luo J, Attard G, de Bono JS. Targeting the androgen receptor pathway in castration-resistant prostate cancer: progresses and prospects. Oncogene 2015;34:1745–57.

36. Carver BS, Chapinski C, Wongvipat J, Hieronymus H, Chen Y, Chandarlapaty S, et al. Reciprocal feedback regulation of PI3K and androgen receptor signaling in PTEN-deficient prostate cancer. Cancer Cell 2011;19:575–86.

37. Meiers I, Waters DJ, Bostwick DG. Preoperative prediction of multifocal prostate cancer and application of focal therapy: review 2007. Urology 2007;70:3–8.

38. Barry M, Perner S, Demichelis F, Rubin MA. TMPRSS2-ERG fusion heterogeneity in multifocal prostate cancer: clinical and biologic implications. Urology 2007;70:630–3.

39. Arora R, Koch MO, Eble JN, Ulbright TM, Li L, Cheng L. Heterogeneity of Gleason grade in multifocal adenocarcinoma of the prostate. Cancer 2004;100:2362–6.

40. Cheng L, Song SY, Pretlow TG, Abdul-Karim FW, Kung HJ, Dawson DV, et al. Evidence of independent origin of multiple tumors from patients with prostate cancer. J Nat Cancer Inst 1998;90:233–7.

41. Pritchard CC, Mateo J, Walsh MF, De Sarkar N, Abida W, Beltran H, et al. Inherited DNA-repair gene mutations in men with metastatic prostate cancer. N Eng J Med 2016;375:443–53.

42. Beltran H, Rickman DS, Park K, Chae SS, Sboner A, MacDonald TY, et al. Molecular characterization of neuroendocrine prostate cancer and identification of new drug targets. Cancer Discov 2011;1:487–95.

43. Lin D, Wyatt AW, Xue H, Wang Y, Dong X, Haegert A, et al. High fidelity patient-derived xenografts for accelerating prostate cancer discovery and drug development. Cancer Res 2014;74:1272–83.

44. Antonarakis ES, Lu C, Luber B, Wang H, Chen Y, Nakazawa M, et al. Androgen receptor splice variant 7 and efficacy of taxane chemotherapy in patients with metastatic castration-resistant prostate cancer. JAMA Oncol 2015;1:582–91.

45. Scher HI, Lu D, Schreiber NA, Louw J, Graf RP, Vargas HA, et al. Association of AR-V7 on circulating tumor cells as a treatment-specific biomarker with outcomes and survival in castration-resistant prostate cancer. JAMA Oncol 2016;2:1441–9.